Supplementary Information (SI) for New Journal of Chemistry.

Supporting Information

Development of Novel AIE-Active Staurosporine-Based Fluorescent Probes with Theranostic Potential

Nannan Chen [a, †], Yuqiu Ye [a, †], Longfeng Zhang [b, †], Xia Wang [a], Shijie Liu [a], Xiaoming Chen [a], Tong Wu [a], Jingming Zhou [a], Haipeng Xu [*, b] and Lijun Xie [*, a]

[a] Fujian Provincial Key Laboratory of Screening for Novel Microbial Products, Fujian Institute of Microbiology, Fuzhou, Fujian 350007, P.R. China.

[b] Clinical Oncology School of Fujian Medical University, Fujian Cancer Hospital, Fuzhou, Fujian 350014, P.R. China.

* Correspondence:

Haipeng Xu Email: penghaixu@163.com

Lijun Xie Emai: lijunxie8224@outlook.com

† These authors contributed equally to this work.

Table of Contents

General experimental information

CCK-8 Assay: First, culture the cells under appropriate conditions (37°C, 5% CO_2, humidity-saturated environment). Once the cells reach the logarithmic growth phase, they are separated and processed. The MCF-7 and NCI-N87 cells are then seeded into flat-bottomed 96-well plates at a density of 7500 cells per well, with 100 μL of complete culture medium, and incubated for 24 hours to allow for adherence and adaptation to the environment. For dark cytotoxicity assessment, after washing the cells three times with PBS, MCF-7 and NCI-N87 cells are incubated with different concentrations (0.1 nM，1 nM，10 nM，100 nM, 1 μM, 10 μM) of Y1, Y2, and Y3. All stock solutions are prepared in DMSO (2 mM) and subsequently diluted with complete medium. After a 24-hour incubation, the cells are washed again with PBS three times. Then, 10 μL of Cell Counting Kit-8 (CCK-8) solution and 90 μL of PBS are added to each well simultaneously. After an additional 1-hour incubation, the absorbance at 450 nm is measured using a 96-well plate reader. Cell viability is calculated based on the absorbance values at different concentrations, with the control group set at 100%. A curve of cell viability versus drug concentration is plotted, and the IC50 value is determined using nonlinear regression analysis.

Fluorescence imaging: First, 100 μL MCF-7 cell suspension was added to 1 mL medium and incubated overnight in a cell incubator. Then the cells were washed with PBS 1-2 times, the drug was mixed into a concentration of 10 μM, and the mixture was mixed according to the ratio of 1 mL: 1 uL (medium solution: drug). After incubation in the incubator for 30 min, the medium was washed once with PBS, and finally 1ml fresh medium was used to replace the medium.

Characterization of STQ

Synthesis of STQ. *Staurosporine* (4.00 g, 8.56 mmol) was dissolved in dichloromethane (240.0 mL) under nitrogen atmosphere and then the solution was transferred to salt ice bath at -15°C. Next, titanium tetrachloride (3.94 g, 34.24 mmol) was added dropwise. Then, dichloromethyl methyl ether (6.50 g, 34.24 mmol) was added dropwise. The reaction was stirred for 0.5 h. After that, the reaction was stirred for another 12 h at room temperature until the reaction was completed. Subsequently, the resulting mixture was poured into ice water, forming a yellow solid that was subsequently filtered to get the crude product. The resultant crude product underwent purification through column chromatography employing dichloromethane and methanol in a 50:1 vol ratio as the eluent. The final product STQ (2.20 g) was obtained as a yellow solid, with a yield of 52.9%. ^{1}H NMR (600 MHz, DMSO-d_6) δ 10.10 (s, 1H), 9.82 (d, J = 1.6 Hz, 1H), 8.66 (s, 1H), 8.04 – 7.95 (m, 3H), 7.79 (d, J = 8.5 Hz, 1H), 7.44 (ddd, J = 8.6, 7.1, 1.3 Hz, 1H), 7.30 (t, J = 7.4 Hz, 1H), 6.80 (dd, J = 5.4, 1.9 Hz, 1H), 4.99 (s, 2H), 4.09 (d, J = 3.6 Hz, 1H), 3.37 (s, 3H), 3.27 (q, J = 3.8 Hz, 1H), 2.56 (ddt, J = 17.8, 9.4, 4.4 Hz, 2H), 2.31 (s, 3H), 1.42 – 1.35 (m, 3H), 0.77 (s, 1H).; ^{13}C NMR (151 MHz, DMSO-d_6) δ 192.1, 171.9, 139.6, 139.4, 133.2, 130.0, 129.6, 128.6, 127.8, 125.5, 124.7, 123.6, 122.5, 121.0, 119.9, 118.9, 115.4, 114.3, 114.3, 109.2, 91.0, 82.7, 80.1, 57.1, 54.9, 49.7, 45.5, 33.2, 29.8, 29.3. HRMS (ESI): calcd for $C_{29}H_{26}N_4O_4$, 495.2027 [M+H]$^+$, found, 495.2039 [M+H]$^+$.

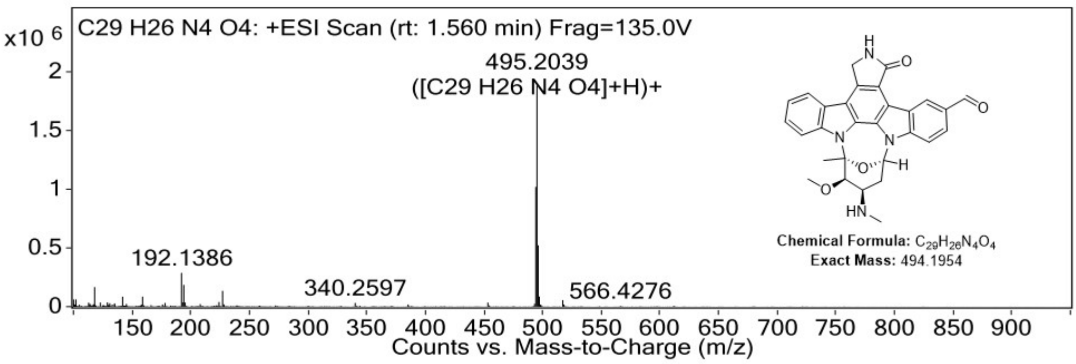

Fig. S1 HRMS spectrum of **STQ**.

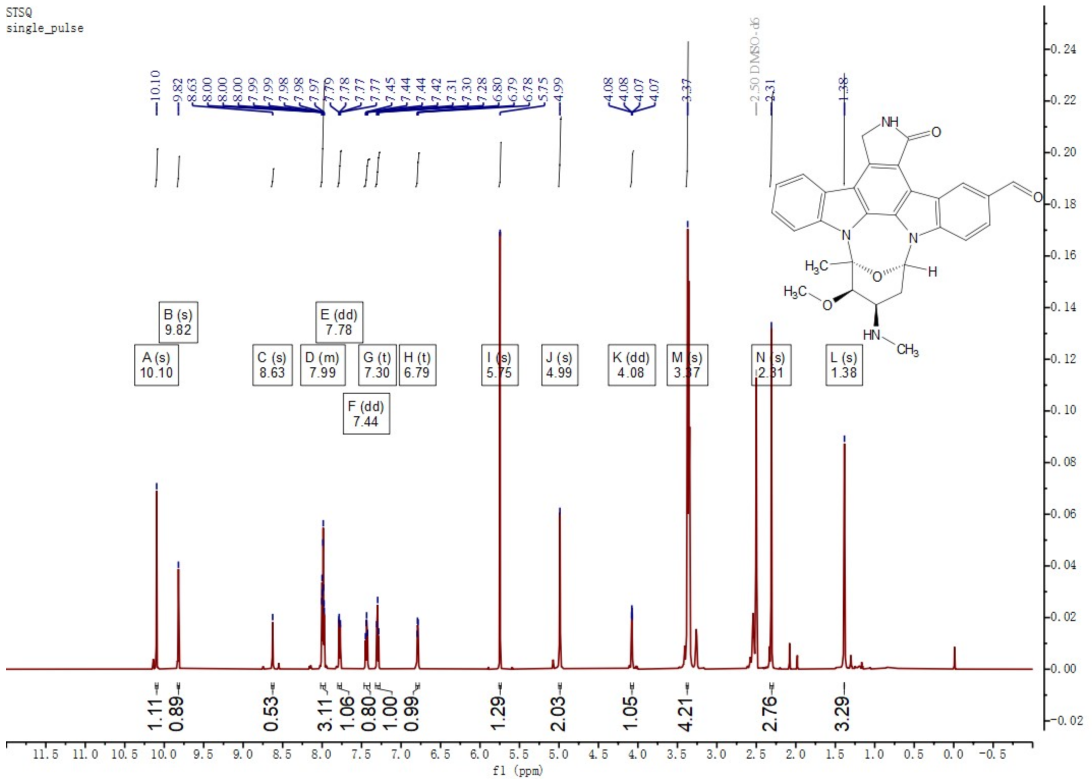

Fig. S2 ^{1}H-NMR spectrum of **STQ** in DMSO-d_6.

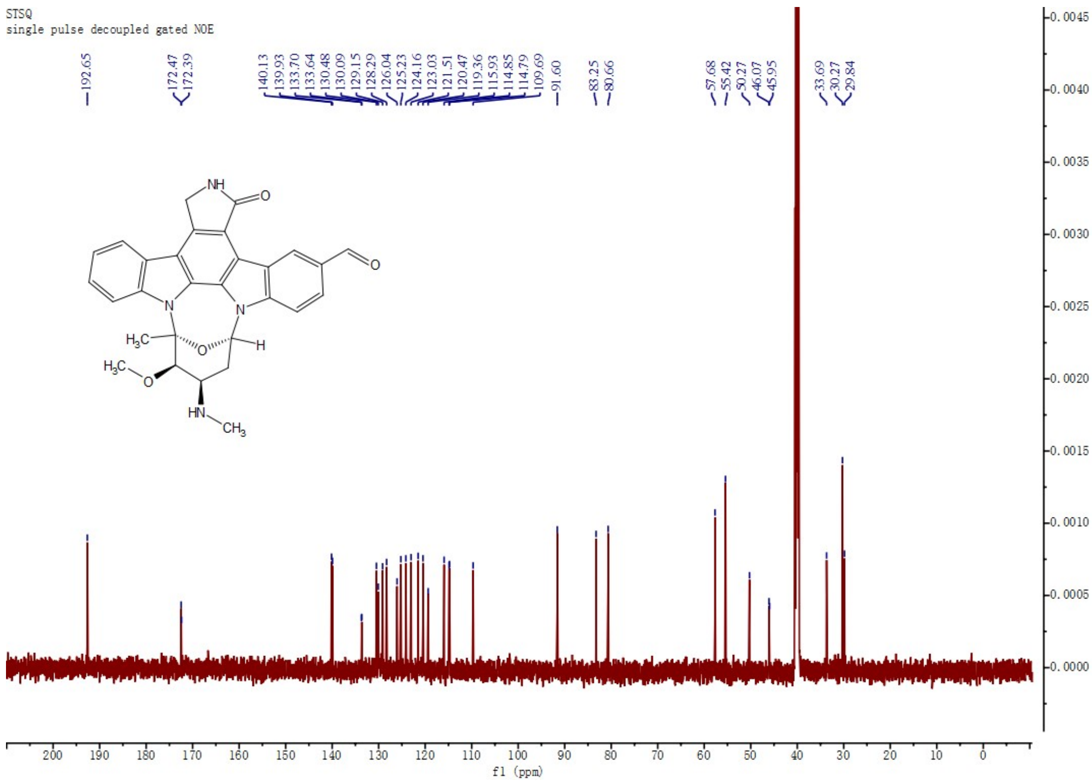

Fig. S3 ^{13}C-NMR spectrum of **STQ** in DMSO-d_6.

Characterization of Y1

Synthesis of Y1. The key intermediate **STQ** (100 mg, 0.20 mmol) was reacted with 4-(trifluoromethyl)phenylacetonitrile (2.0 mmol) in ethanol (5 mL) using sodium hydroxide (8 mg, 0.2 mmol) as a base. The reaction mixture was stirred at room temperature for 12 hours in the absence of light. After completion of the reaction, confirmed by TLC analysis, the resulting precipitate was collected via filtration. The solid was subsequently washed with water and ethanol to yield the pure product, which was then dried under reduced pressure to give the orange- yellow powder **Y1** (113.6 mg) with the yield 85.1%. ^{1}H NMR (600 MHz, DMSO-d_6) δ 9.75 (d, J = 1.9 Hz, 1H), 8.61 (s, 1H), 8.32 (s, 1H), 8.27 (dd, J = 8.8, 1.9 Hz, 1H), 8.04 (d, J = 8.1 Hz, 2H), 8.01 - 7.97 (m, 2H), 7.87 (d, J = 8.1 Hz, 2H), 7.81 (t, J = 8.3 Hz, 2H), 7.46 – 7.39 (m, 1H), 7.32 – 7.26 (m, 1H), 6.81 – 6.77 (m, 1H), 4.98 (s, 2H), 4.09 (d, J = 3.5 Hz, 1H), 3.37 (s, 4H), 3.27 (q, J = 3.8 Hz, 1H), 2.62 – 2.52 (m, 2H), 2.31 (s, 3H), 1.41 (s, 4H), 0.81 (s, 1H). ^{13}C NMR (151 MHz, DMSO-d_6) δ 171.9, 147.0, 139.6, 138.7, 137.5, 132.9, 130.0, 129.7, 129.6, 127.6, 126.3, 126.1, 126.1, 124.9, 124.7, 124.6, 123.7, 122.8, 121.0, 119.9, 119.0, 118.3, 115.4, 114.2, 114.1, 109.2, 105.2, 91.1, 91.1, 82.8, 80.1, 57.2, 49.8, 45.5, 33.3, 33.3, 29.8, 29.4. HRMS (ESI): calcd for $C_{38}H_{31}F_3N_5O_3$, 662.2374 $[M+H]^+$, found: 662.2383 $[M+H]^+$.

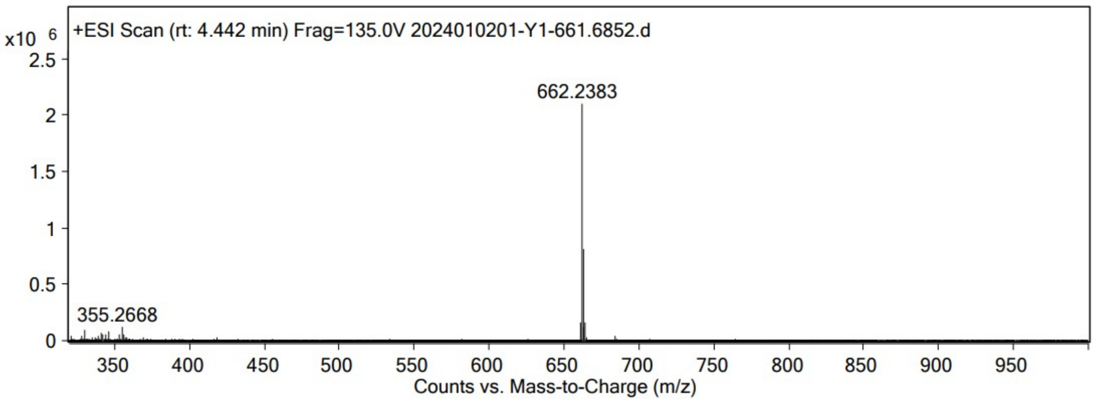

Fig. S4 HRMS spectrum of **Y1**

.

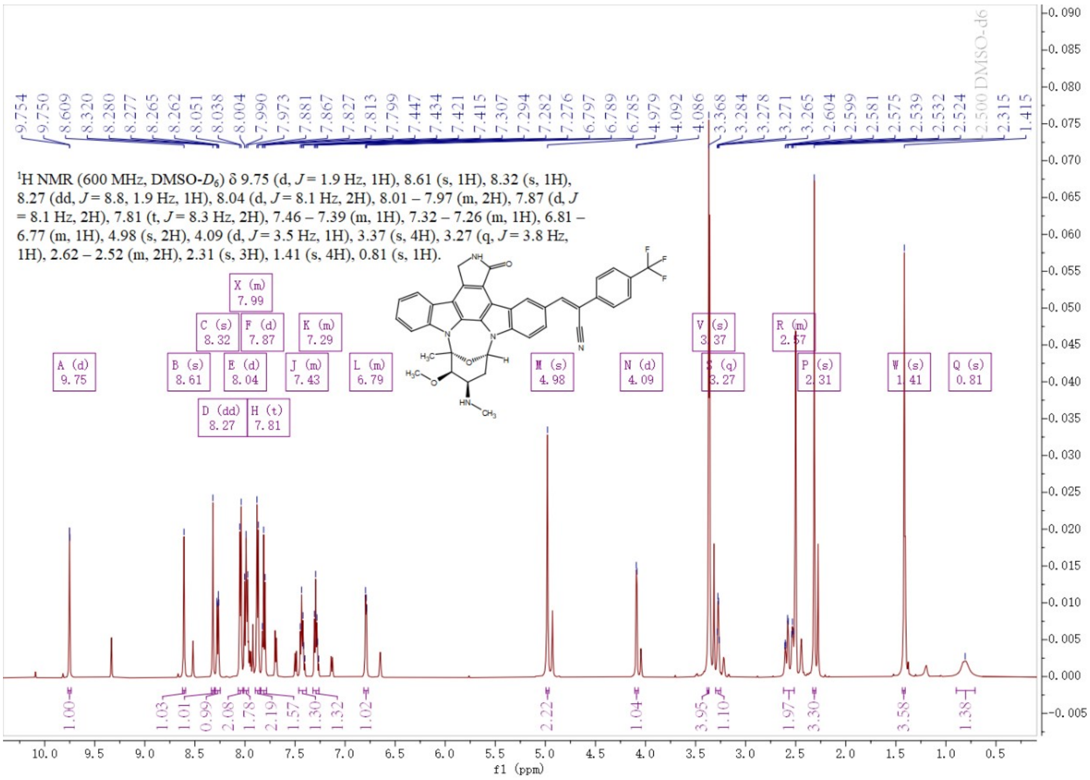

Fig. S5 ^{1}H-NMR spectrum of **Y1** in DMSO-d_6.

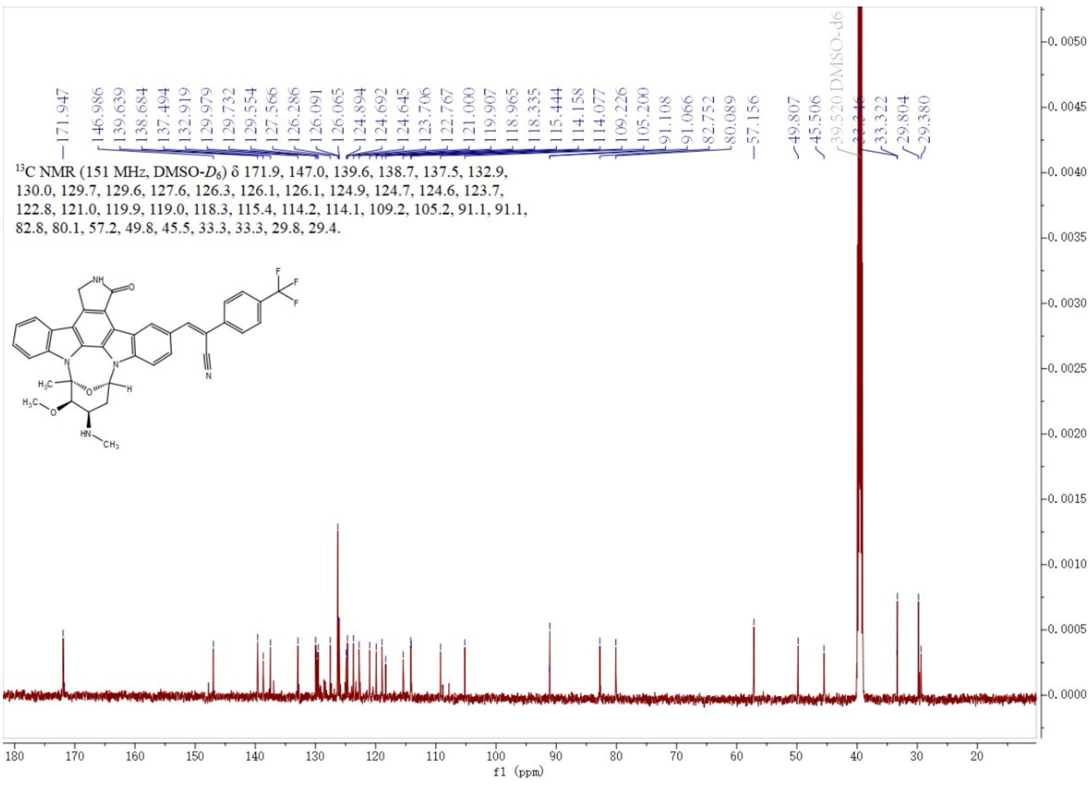

Fig. S6 ^{13}C-NMR spectrum of **Y1** in DMSO-d_6.

Characterization of Y2

Synthesis of **Y2**. The synthetic procedure is the same as that of Y1, except using 4-chlorophenylacetonitrile instead of 4-(trifluoromethyl)phenylacetonitrile. Orange-yellow powder **Y2** (111.3 mg) with the yield 87.6%. ^{1}H NMR (600 MHz, DMSO-d_6) δ 9.71 (s, 1H), 8.60 (s, 1H), 8.22 (d, J = 8.7 Hz, 1H), 8.19 (s, 1H), 7.99 (t, J = 9.3 Hz, 2H), 7.84 (d, J = 8.2 Hz, 2H), 7.79 (d, J = 8.7 Hz, 1H), 7.58 (d, J = 8.2 Hz, 2H), 7.43 (t, J = 7.8 Hz, 1H), 7.29 (t, J = 7.3 Hz, 1H), 6.78 (d, J = 5.4 Hz, 1H), 4.98 (s, 2H), 4.08 (d, J = 3.5 Hz, 1H), 3.36 (s, 3H), 3.27 (s, 1H), 2.61 - 2.52 (m, 2H), 2.31 (s, 3H), 1.41 (d, J = 5.9 Hz, 3H), 0.78 (q, J = 6.7 Hz, 1H). ^{13}C NMR (151 MHz, DMSO-d_6) δ 172.0, 145.3, 139.6, 137.3, 133.5, 133.1, 132.8, 130.0, 129.2, 129.1, 127.5, 127.3, 124.9, 124.7, 124.6, 123.7, 122.7, 121.0, 119.9, 119.0, 118.4, 115.4, 114.1, 114.1, 109.1, 105.6, 91.1, 82.8, 80.1, 57.2, 49.8, 45.5, 33.3, 29.8, 29.4, 0.1. HRMS (ESI): calcd for $C_{37}H_{31}ClN_5O_3$, 628.2110 $[M+H]^+$, found: 628.2114 $[M+H]^+$.

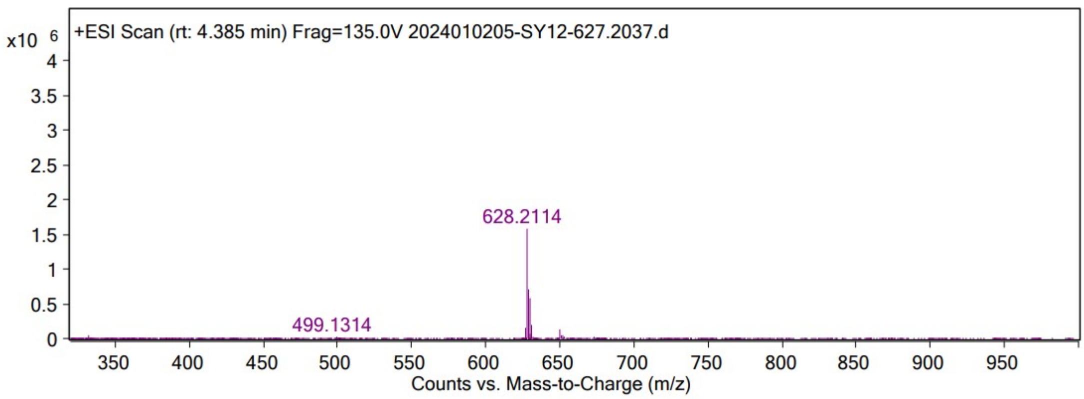

Fig. S7 HRMS spectrum of **Y2**.

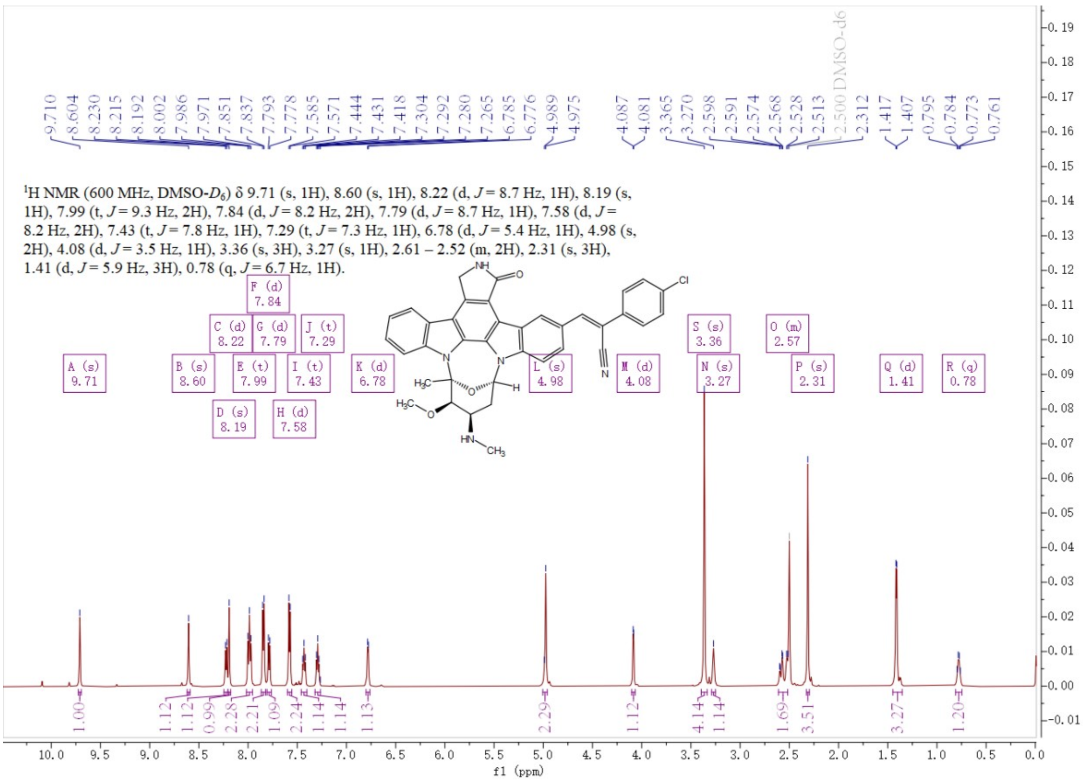

Fig. S8 ^{1}H-NMR spectrum of **Y2** in DMSO-d_6.

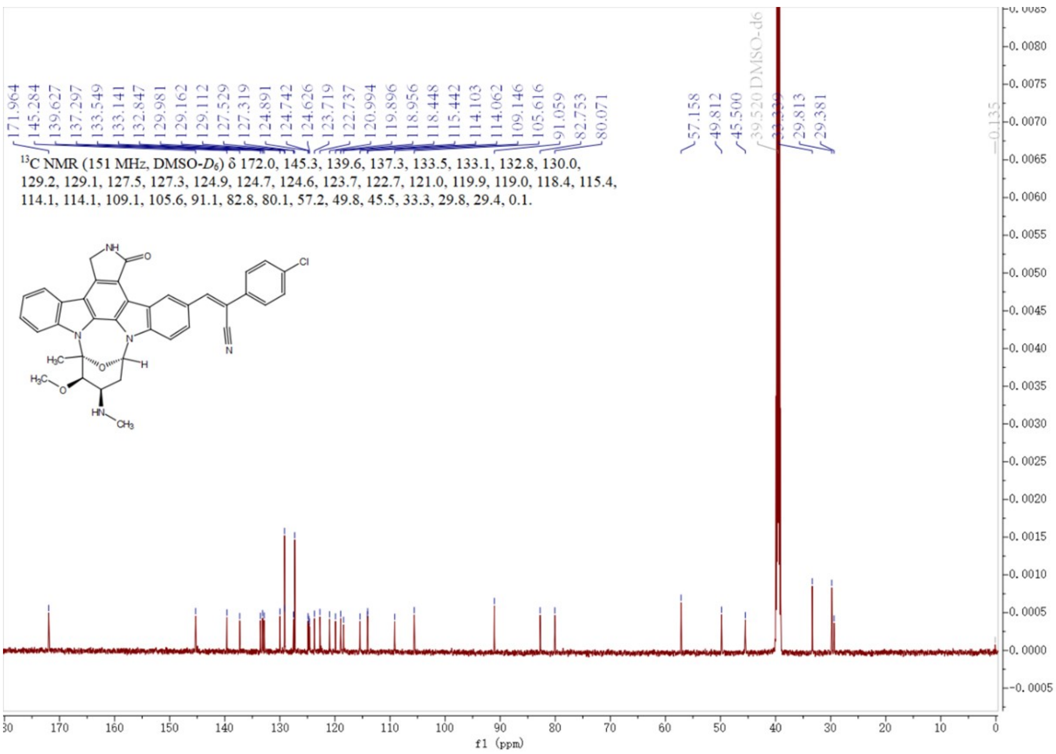

Fig. S9 ^{13}C-NMR spectrum of **Y2** in DMSO-d_6.

Characterization of Y3

Synthesis of **Y3**. The synthetic procedure is the same as that of Y1, except using 4-biphenylacetonitrile instead of 4-(trifluoromethyl)phenylacetonitrile. Orange- yellow powder **Y3** (100.2 mg) with the yield 74.2%. ^{1}H NMR (600 MHz, DMSO-d_6) δ 9.75 (s, 1H), 8.62 (s, 1H), 8.26 (d, J = 8.6 Hz, 1H), 8.22 (s, 1H), 7.99 (dd, J = 11.8, 8.1 Hz, 2H), 7.89 (d, J = 7.9 Hz, 2H), 7.80 (d, J = 8.3 Hz, 3H), 7.72 (d, J = 7.5 Hz, 2H), 7.48 (t, J = 7.7 Hz, 2H), 7.44 (t, J = 7.7 Hz, 1H), 7.39 (t, J = 7.4 Hz, 1H), 7.30 (t, J = 7.3 Hz, 1H), 6.79 (d, J = 5.4 Hz, 1H), 4.98 (s, 2H), 4.08 (d, J = 3.4 Hz, 1H), 3.37 (s, 4H), 3.27 (d, J = 4.5 Hz, 1H), 2.62 – 2.51 (m, 2H), 2.31 (s, 3H), 1.41 (d, J = 5.7 Hz, 3H), 0.76 (d, J = 6.9 Hz, 1H). ^{13}C NMR (151 MHz, DMSO-d_6) δ 172.0, 144.4, 140.1, 139.6, 139.1, 137.2, 133.6, 132.8, 130.0, 129.1, 129.0, 127.9, 127.5, 127.3, 126.6, 126.1, 125.1, 124.8, 124.6, 123.7, 122.8, 121.0, 119.9, 119.0, 118.7, 115.5, 114.1, 109.1, 106.4, 91.1, 82.8, 80.1, 57.1, 49.8, 45.5, 33.3, 29.8, 29.4. HRMS (ESI): calcd for $C_{43}H_{36}N_5O_3$, 670.2813 $[M+H]^+$, found: 670.2820 $[M+H]^+$.

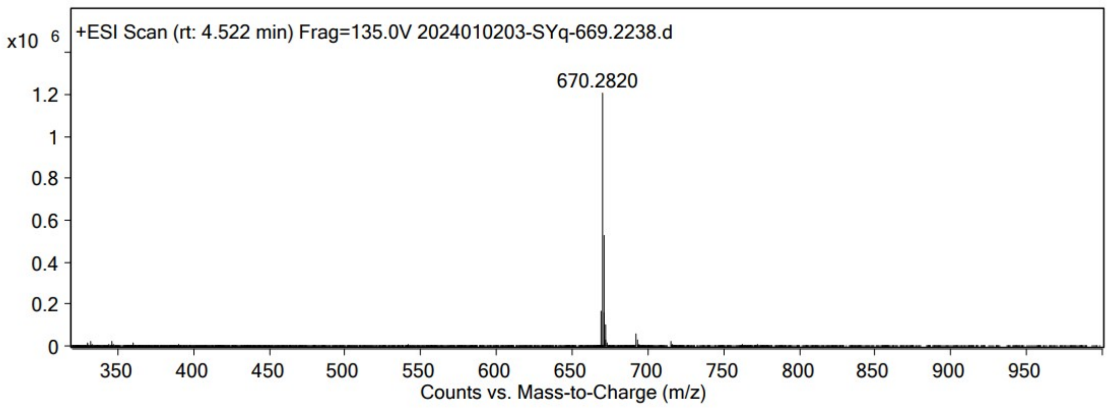

Fig. 10 HRMS spectrum of **Y3**

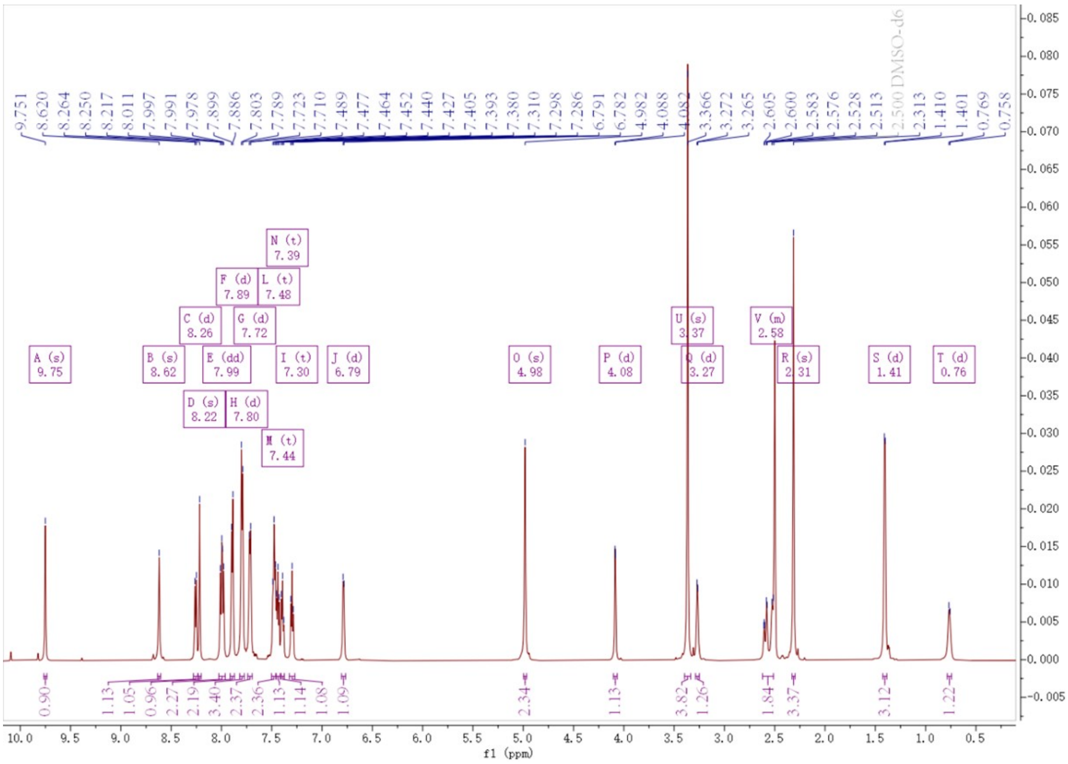

Fig. 11 ^{1}H-NMR spectrum of **Y3** in DMSO-d_6.

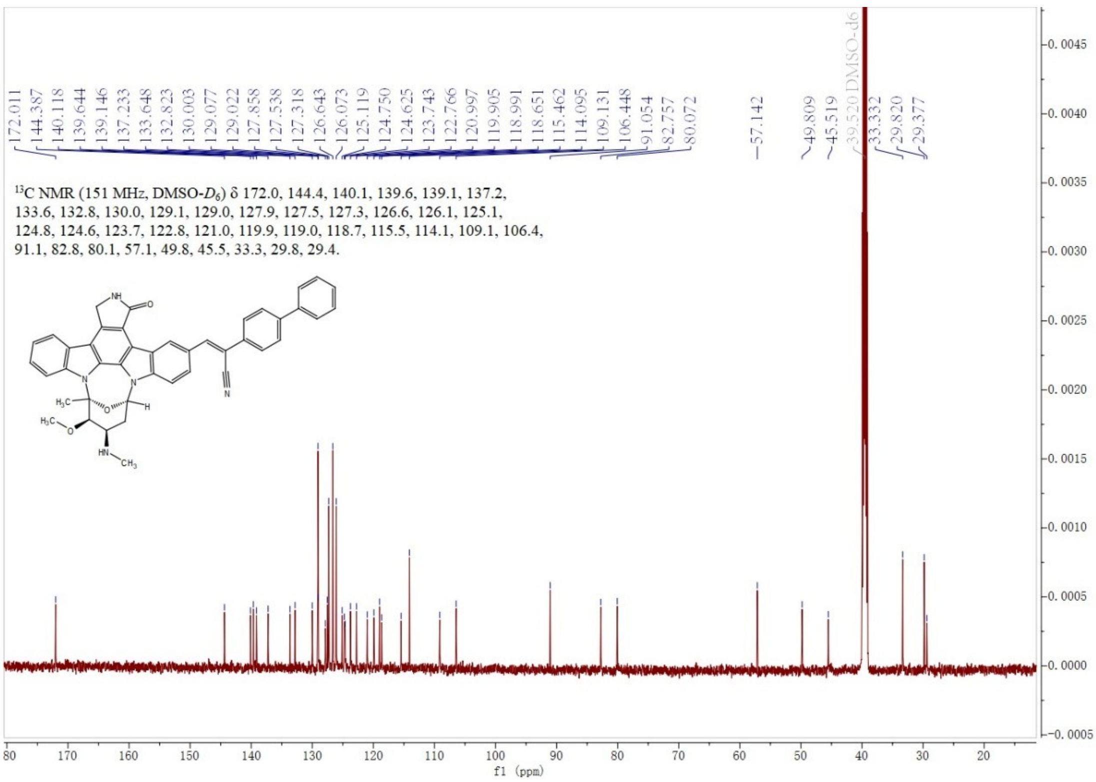

Fig. 12 ^{13}C-NMR spectrum of **Y3** in DMSO-d_6.

The absorption of compounds in DMSO/H_2O mixture

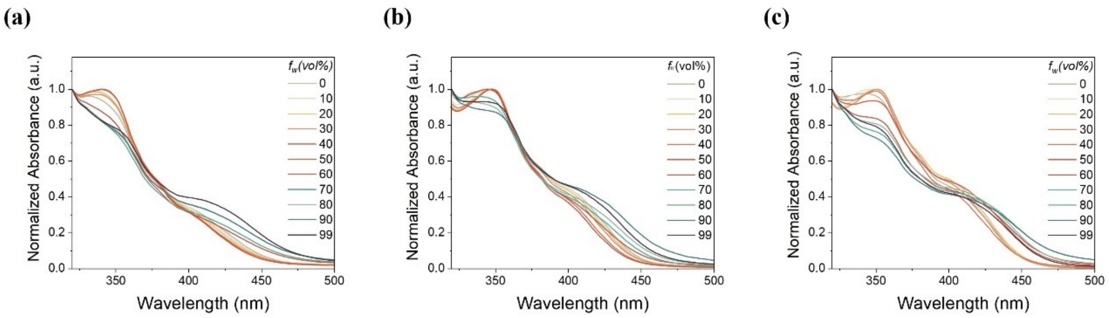

Fig. S13 Absorption spectra of **Y1** (a), **Y2** (b) **and Y3** (c) in DMSO/H_2O mixture with different f_w (1.0×10^{-5} mol L^{-1}).

Fluorescence emission spectra of compounds in DMSO/glycerol mixture

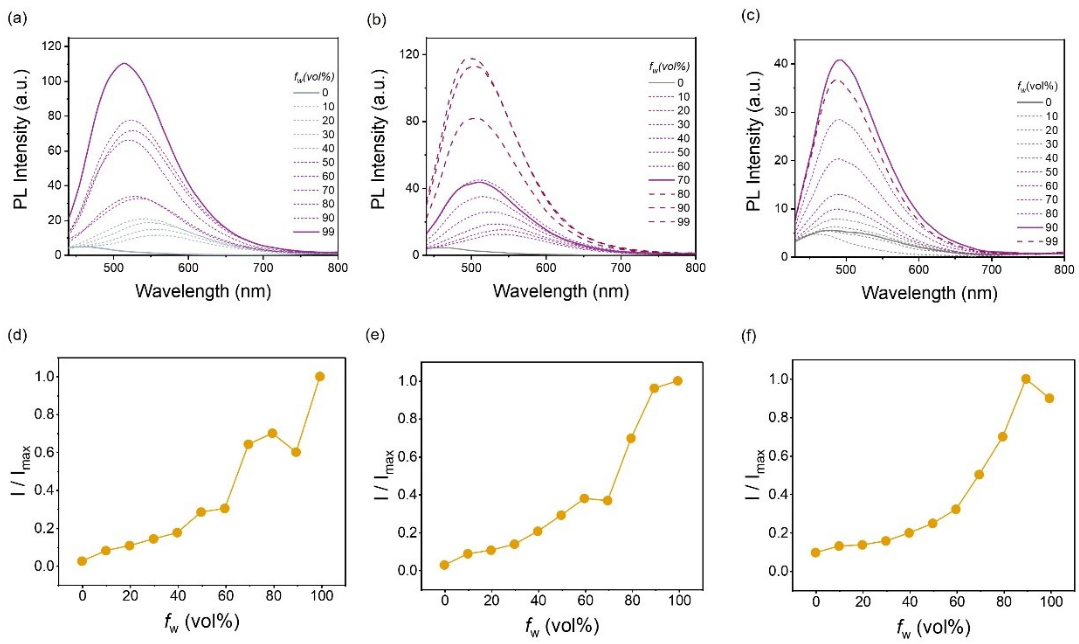

Fig. S14 Fluorescence emission spectra of (a) **Y1**, (b) **Y2** and (c) **Y3** in pure DMSO with increasing glycerol fractions. Plots of FL emission intensity (I/I_{max}) versus the composition of the DMSO/glycerol mixture of (d) **Y1**, (e) **Y2** and (f) **Y3**.

The absorption spectral and emission spectral of STQ in DMSO/H_2O mixture

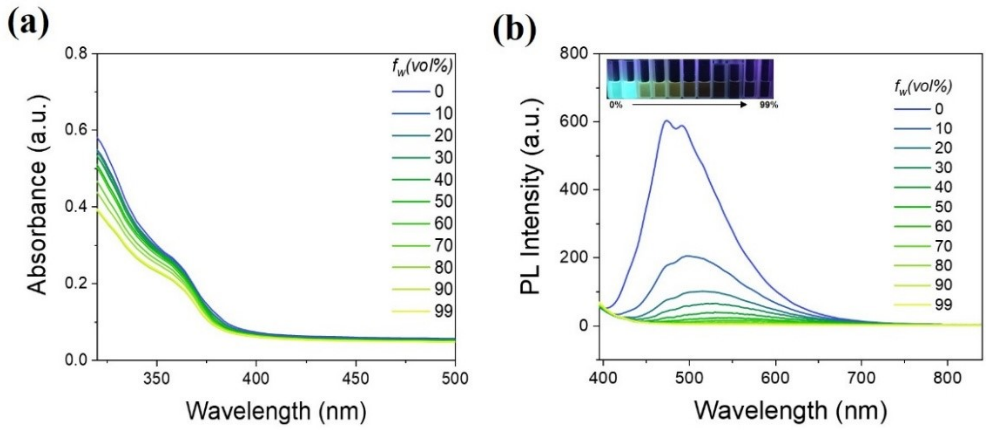

Fig. S15 (a) Absorption spectra of **STQ** in DMSO/H_2O mixture with different $f_{w.}$ (b) The FL spectra of **STQ** in pure DMSO with increasing water fractions. (Inset: photographs of **STQ** in different DMSO/H_2O mixtures under 365 nm hand-held UV lamp irradiation).

Absorption spectral of Y1, Y2 and Y3 in various solvents

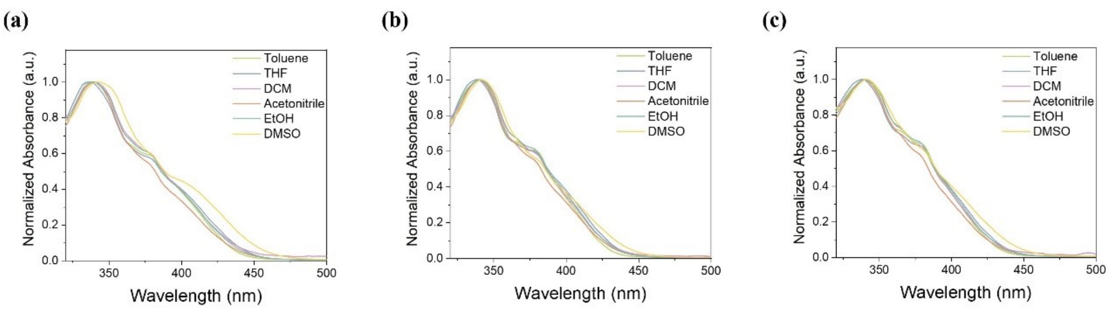

Fig. S16 UV-vis absorption spectra of **Y1** (a), **Y2** (b) and **Y3** (c) (5×10^{-5} mol/L) in different solvents.

Lippert–Mataga plot for Y1, Y2 and Y3 in various solvents

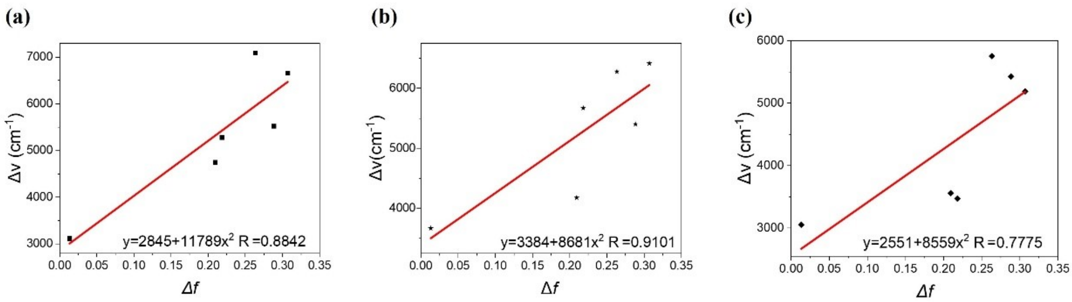

Fig. S17 Lippert–Mataga plot for **Y1** (a), **Y2** (b) and **Y3** (c) in various solvents.

Table S1. Photophysical Properties of Compounds in different solvents (50 μM).

Compd.		Toluene	THF	DCM	ACN	EtOH	DMSO
Y1	λ_{abs}(nm)[a]	338	336	340	340	340	342
	λ_{em}(nm)[b]	472	508	522	560	532	586
	$\triangle\lambda$(nm)[c]	134	172	182	220	192	244
	$\triangle V$(cm^{-1})[d]	8399	10077	10255	11555	10615	12175
Y2	λ_{abs}(nm)[a]	340	338	340	340	340	342
	λ_{em}(nm)[b]	522	518	520	540	518	552
	$\triangle\lambda$(nm)[c]	182	180	180	200	178	210
	$\triangle V$(cm^{-1})[d]	10255	10281	10181	10893	10107	11124
Y3	λ_{abs}(nm)[a]	342	338	340	340	340	342
	λ_{em}(nm)[b]	462	480	476	530	522	536
	$\triangle\lambda$(nm)[c]	120	142	136	190	182	194
	$\triangle V$(cm^{-1})[d]	7595	8752	8403	10544	10255	10583

[a] the maximum absorption wavelength;[b] the maximum emission wavelength;[c] the value of stokes shift; [d] Δv were calculated using the equation $(1/\lambda_{abs}-1/\lambda_{em})\times10^{7}$.

Density Functional Theory (DFT) Calculations

Density functional theory (DFT) calculations were performed using Gaussian 09 software at the B3LYP/6-311G level with the implicit solvent model (SMD, DMSO). The optimized geometries and electronic structures of the compounds were first obtained at the B3LYP/6-31G level, incorporating D3 dispersion correction.

Table S2. TD-DFT calculations using the SMD model to evaluate emission transitions of Y1 in toluene and DMSO

Solvents	Excited State	E_g (eV)[a]	λ_{em} (nm)[b]	f (oscillator strengths)
Toluene	$S_0 \rightarrow S_1$	2.80	443	0.70
DMSO	$S_0 \rightarrow S_1$	2.70	460	0.92

[a] Energy gap between S_0 and S_1; [b] the maximum emission wavelength